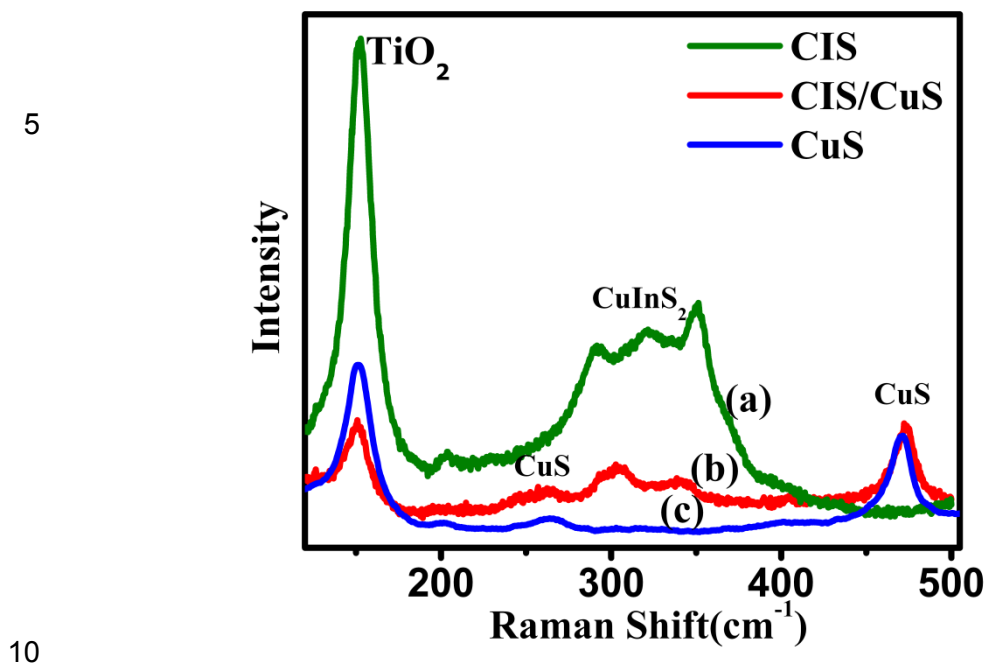
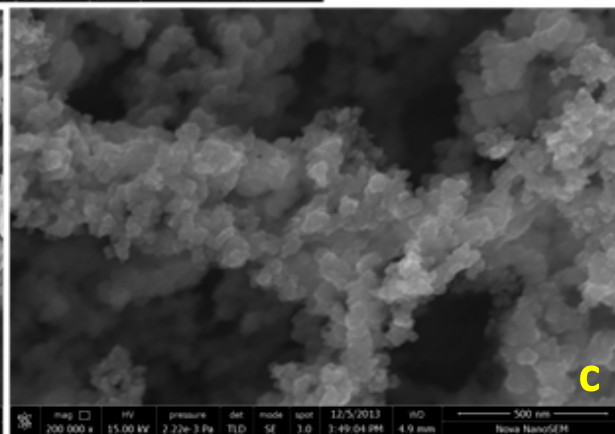
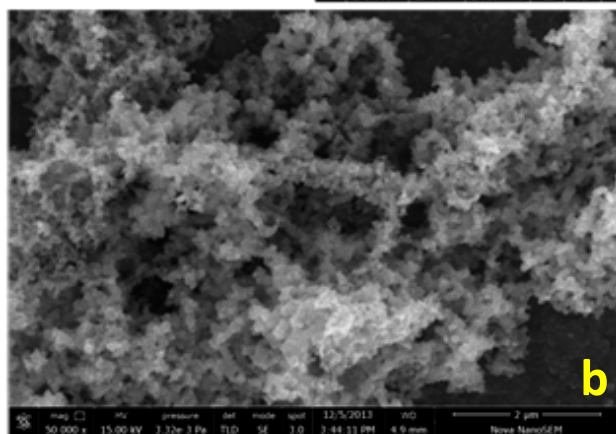
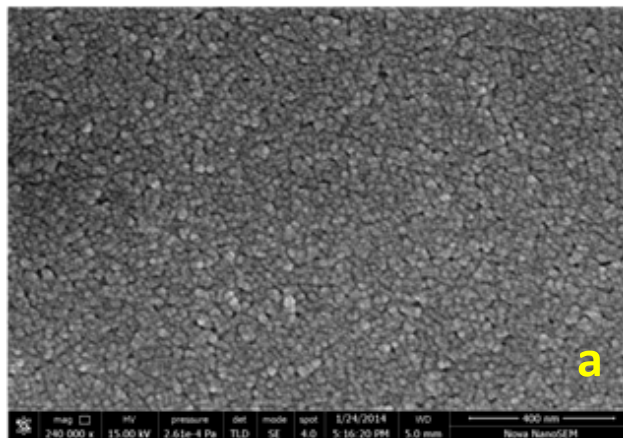


## Supplementary Information



**SI-I:** Raman spectra of CIS film (a) annealed at 500<sup>o</sup>C (b) annealed at 250<sup>o</sup>C and (c) pure CuS film

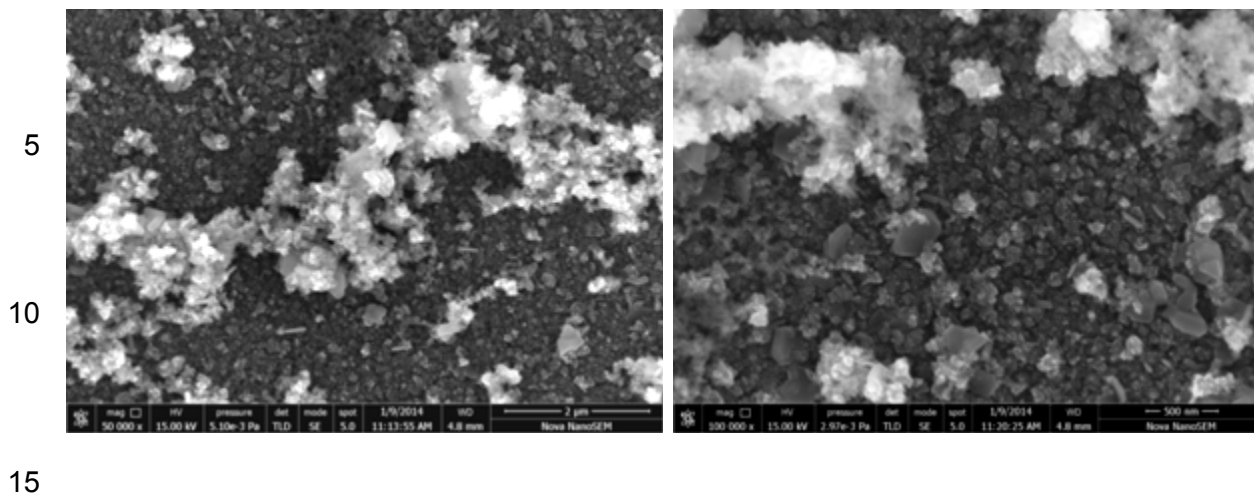
5



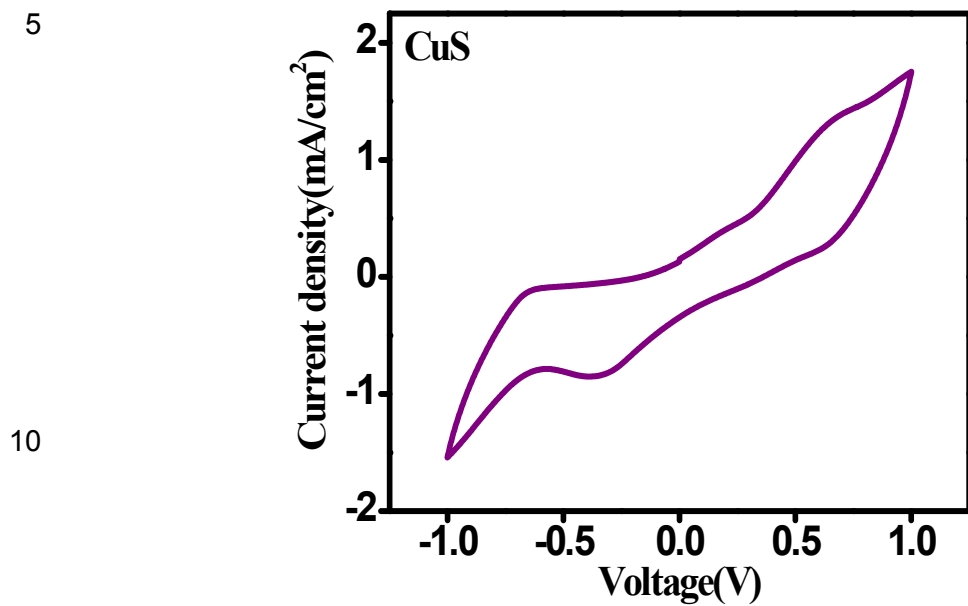
10

SI-II FESEM images of (a) TiO<sub>2</sub> film (b, c) CuS on TiO<sub>2</sub> coated FTO

15



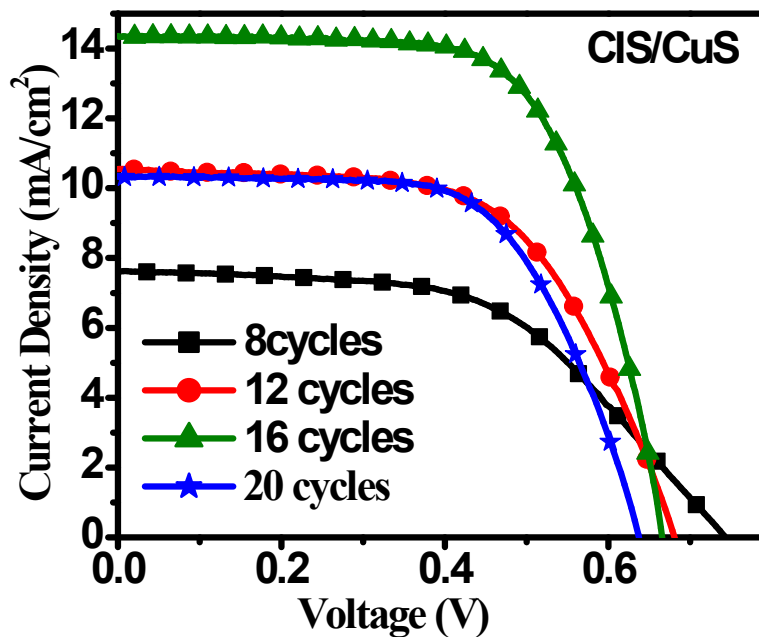
**SI-III** FESEM images of CIS on FTO without TiO<sub>2</sub>



SI-IV Cyclic voltametry data of CuS counter electrode

15

**SI-V Photovoltaic performance**



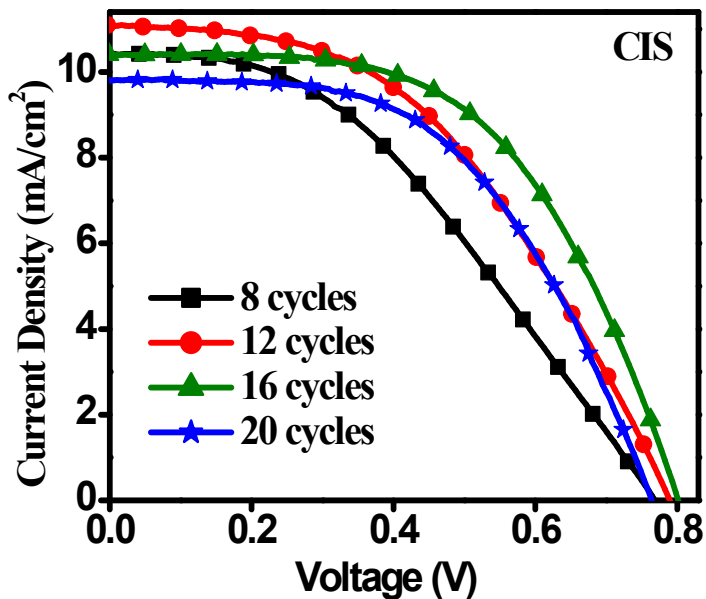
5

Sample	$V_{oc}$ (V)	$J_{sc}$ (mA/cm <sup>2</sup> )	FF (%)	Efficiency (%)
8cycles	0.74	7.6	54	3.2
12 cycles	0.68	10.5	60	4.6
16 cycles	0.70	14.4	66	6.3
20 cycles	0.64	10.2	63	4.5

10

**SI-V:** I-V data of CIS/CuS as counter electrodes at different SILAR cycles

5



10

Sample	$V_{oc}$ (V)	$J_{sc}$ (mA/cm <sup>2</sup> )	FF (%)	Efficiency (%)
8cycles	0.76	10.4	40	3.5
12 cycles	0.78	11.0	46	4.4
16cycles	0.80	10.5	55	5.0
20 cycles	0.76	9.8	53	4.3

SI-VI: I-V data of CIS as counter electrodes at different SILAR cycles

### SI VII *Proposed Mechanism:*

To study the formation mechanism of CIS nanosheets, only FTO and FTO coated TiO<sub>2</sub> were studied in detail, the latter to also concurrently investigate the role of TiO<sub>2</sub> nanoparticles in the specific morphology evolution. The thin film of TiO<sub>2</sub> increases the roughness of surface and thereby the adhesive anchoring of CIS nanosheets on it. Also hydrophilicity of TiO<sub>2</sub> surface promote nucleation as the hydroxyl groups present on the TiO<sub>2</sub> surface bond with metal cations, such as Cu<sup>2+</sup> and In<sup>3+</sup> and control random crystal aggregation.<sup>1</sup> When this TiO<sub>2</sub> modified FTO is dipped in solutions for SILAR process, it undergoes heterogenous nucleation. In SILAR, ions from precursors go ion-by-ion adsorption directly on the substrate forming CIS nuclei. Thus the reactants are transported from the solution to the solution/substrate interface, leading to the deposition on the substrate and further crystal growth. Therefore, it is more convenient for the nucleation and adhesion of CuInS<sub>2</sub> seeds on the rough TiO<sub>2</sub> surface, due to the lower interfacial energy between the substrate and the solution. A control experiment was also performed without coating of TiO<sub>2</sub> on FTO which gave rise to poor coverage of material on FTO. Moreover FESEM images revealed that there is formation of CIS nanoparticle clusters with random growth. This is due to the lesser hydrophilic property of FTO than TiO<sub>2</sub>. Thus TiO<sub>2</sub> not only promotes adhesion of CIS film but also gives rise to unique morphology of nanosheets.

With further increase in the SILAR cycles, crystal growth continues by consumption of more reactants. Thus the morphology is strictly dependent on the concentration of reactants and dipping time of substrates in solutions. After the nucleation step, CIS nuclei undergo *in situ* anisotropic growth process forming thin nanosheets perpendicular to substrate. This phenomenon could be explained by “evolutionary selection” mechanism proposed by Van der Drift<sup>2,3</sup> which means that only the facets with the highest growth rate and perpendicular to the growth surface would be favorable to the crystal growth. This concurrent growth of a large number of CIS nanosheets form a net or mesh like system to reduce the surface energy of the system. With further increase in the cycles these coalescence of

nanosheets undergoes self-assembly process to form channels of nanoplates interconnected with each other. This is evident from the TEM images in Fig (5) where uniform plate-like structures display clear nanosheet edges.

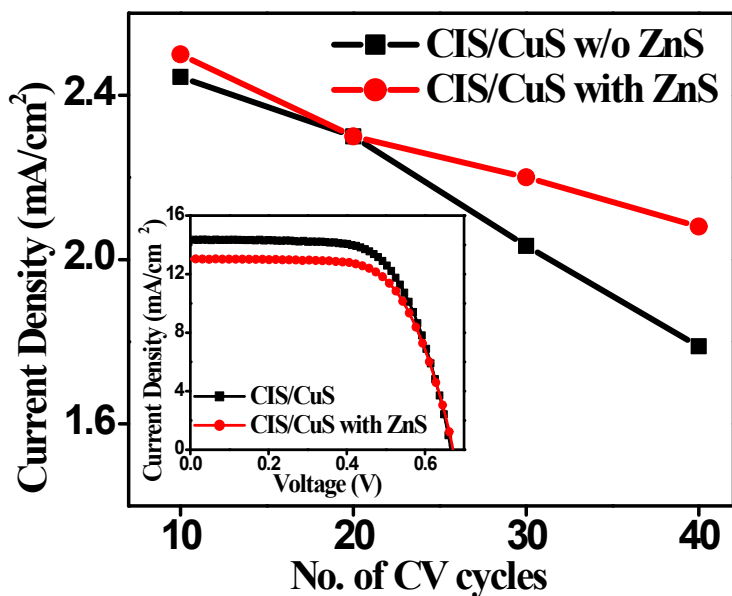
As prepared CIS is amorphous in nature. Upon annealing at 250°C some of the unreacted ions of Cu<sup>2+</sup> and from solution or ions from stoichiometric CIS, oozing out of the film cause CuS aggregation. It is well known that the solution method is based on surface chemistry through changing the interfacial tension to control the structure and morphology of the products, but at higher temperature the chemical kinetics of diffusion of dissolved reactants is enhanced.<sup>3</sup> Therefore the higher temperature could induce secondary nucleation favoring dissolution of unreacted ions and of thinner nanosheets to form thicker ones according to the nucleation–dissolution–recrystallization mechanism. During this mechanism binary products may come out giving rise to temperature induced composite. In 500°C case same is the situation but it is an ideal temperature reported by many reports, where all the unreacted ions diffuse to form pure chalcopyrite CIS with no secondary phase. From the FESEM it is clear that nanosheets are more fused compared to the 250°C annealed case due to grain boundary diffusion.



SI-VIII

Stability data

5



10

Name	V <sub>oc</sub> (V)	J <sub>sc</sub> (mA/cm <sup>2</sup> )	FF %	η %
CIS/CuS	0.67	14.4	66.3	6.3
CIS/CuS with ZnS	0.67	13.0	66.4	5.8

SI-VIII: Stability data with I-V data as inset of CIS/CuS counter electrode with and without ZnS layer.

In order to protect the counter electrodes from corrosion of iodine a surface passivation layer of ZnS 15 (0.2M) was deposited on the CIS/CuS (250°C annealed) counter electrode (the best performer) by SILAR method. It can be seen that the stability of the ZnS coated electrode is better than the one without ZnS. Inset shows the I-V data which reflects the effect of ZnS coating on the device performance. The ZnS coated counter electrode device shows slightly lower efficiency but enhanced stability. Further work is clearly needed to solve this issue.

20

## References

- 1) S. Peng, Y. Wu, P. Zhu, V. Thavasi, S. Ramakrishna, S. Mhaisalkar, *J. Mater. Chem.*, 2011, **21**, 15718-15726.
- 2) V. Drift, “Evolutionary Selection, A Principle Governing Growth Orientation in Vapour-  
5 Deposited Layers”. *Philips Res. Rep.* 1967, **22**, 267-288.
- 3) S. Peng, P. Zhu, V. Thavasi, S. Mhaisalkar , S. Ramakrishna, *Nanoscale* ,2011, **3**, 2602- 2608.